Qing LI[1], Gehao SHENG[2], Yadong LIU[2], Wubing QIU[1], Kaisui CAI[1], Xingquan HUANG [1], Xiuchen JIANG[2]

Electric Power Research Institute of Henan(1), Shanghai Jiao Tong University(2)

Research of the GIS Structure Influence on Propagation Characteristic of Partial Discharge Electromagnetic Waves

Abstract. *Partial discharge process caused by Gas Insulatd Switchgear (GIS) typical insulation defect is mainly analyzed in this study, and propagation properties of electromagnetic waves in actual GIS structure are investigated by applying FDTD algorithm and using real PD current signal as excitation source. The results show that great difference occurs between electromagnetic waves excited by PD actual current signal and that by ideal Gaussian pulse excitation and basin type insulator, shielding electrodes and three-phase common enclosure can affect the amplitude, frequency component and propagation mode of electromagnetic waves. The electromagnetic waves signal intensity is not necessarily proportional to its distance from discharge source; the proportion of frequency components is proportional to the diameter of GIS shell when it propagate in breakers .*

Streszczenie. *Zaprezentowano stadium wyładowania niezupełnego przy typowych defektach łączników gazowych. Zastosowano metodę różnic skończonych. Zaobserwowano istotne różnice fali elektromagnetycznej przy rzeczywistym wyładowaniu w stosunku do modelu teoretycznego. Sygnał fali elektromagnetycznej jest proporcjonalny do średnicy powłoki wyłącznika. (**Badania wpływu struktury wyłącznika gazowego na propagację fali elektromagnetycznej przy wyładowaniu niezupełnym**)*

Keywords: PD; propagation of electromagnetic Waves; Gas Insulatd Switchgear(GIS); basin type insulator ; shielding electrode ; breaker
Słowa kluczowe: wyładowanie niezupełne, wyłącznik gazowy.

Introduction

Partial discharge(PD) current pulse in Gas Insulatd Switchgear(GIS) possesses steep rising edge, with the rising time of ns order[1-2], and the electromagnetic waves with the frequency of GHz excited propagates in the coaxial structure formed by GIS cavity. Due to the coaxial structure of GIS, the electromagnetic wave not only propagates in the form of transverse electromagnetic wave (e.g. TEM wave), but also in the form of high-order mode wave, namely, transverse electric wave and transverse magnetic wave. TEM wave is non-dispersion wave, and it can propagate in GIS at any frequency. When frequency f > 100MHz, rapid attenuation occurs along the propagation direction; however, TM wave differs from TE wave in that they have their respective cut-off frequency f_c which is related with the size of GIS. It means that the larger the cross-sectional area of GIS, the lower f_c is. If signal frequency $f < f_c$, the attenuation of signals is so rapid that they cannot propagate any more; when $f > f_c$, signals can propagate without loss basically. Meanwhile, the connection cavity of GIS bus bar can be treated as coaxial resonator cavity on the UHF wave band, and the resonance duration of electromagnetic wave is generally tens of us orders, with its maximum of over 10ms[3]. Inside GIS, there are high-voltage conductors, joints, shields and basin type insulator, etc; its structure can be classified into straight tube, L branch and T branch. Because of different locations of PD generation, the propagation and resonance mode of electromagnetic waves in GIS are very complex.

However, excitation source currently used in the research on this specific field is ideal Gaussian pulse characterized by smooth waveform and bilateral symmetry, which is not completely consistent with actual waveform of current of partial discharge [4-7]. So far, there has been no literature about the research of propagation of electromagnetic waves with real PD current pulse as excitation source. Therefore, real PD current signal with various insulation defects is used as excitation source in this study. Considering the actual internal structure of GIS, electromagnetic simulation software XFDTD 6.3.8.4 should be applied in the study on propagation properties of electromagnetic waves inside GIS.

Propagation properties of electromagnetic waves in GIS partial discharge using real current signal as excitation source

FDTD algorithm

Maxwell's Equations incorporates all the information concerning the description of the properties of the electromagnetic waves at an arbitrary point in the medium. If electromagnetic waves exist, four Maxwell's Equations have to be satisfied at the source point, at an arbitrary point in their propagation medium, and in the loading of them being received or absorbed. Passive homogenous medium is considered, with electric permittivity of ε, magnetic permeability of μ, electric conductivity of σ, electric field of E, and magnetic field of H. Then Maxwell' Equations are expressed as follows:

$$\nabla \times \vec{E} = -\mu \frac{\partial \vec{H}}{\partial t} \tag{1}$$

$$\nabla \times \vec{H} = \sigma \vec{E} + \varepsilon \frac{\partial \vec{E}}{\partial t} \tag{2}$$

$$\nabla \cdot \vec{B} = 0 \Rightarrow \nabla \cdot \vec{H} = 0 \tag{3}$$

$$\nabla \cdot \vec{D} = 0 \Rightarrow \nabla \cdot \vec{E} = 0 \tag{4}$$

Where: $\vec{B} = \mu \vec{H}$, $\vec{D} = \varepsilon \vec{E}$.

First, Maxwell's curl equations are generated into six equations with scalar field components in rectangular coordinate system, then, the solution space is divided into several grid cells along three axes. Each unit length is served as space variable, thus obtaining corresponding time variable. Limited difference equation is used to express the differential of field component to space and time variables, and FDTD basic equation is obtained.

Supposing that the space researched is passive, and medium parameters ε , μ , σ and s are constants. In Cartesian coordinate system, Maxwell's Equations can be converted into six scalar equations:

$$\frac{\partial H_z}{\partial y} - \frac{\partial H_y}{\partial z} = (\sigma + \varepsilon \frac{\partial}{\partial t}) E_x \tag{5}$$

(6) $$\frac{\partial H_x}{\partial z}-\frac{\partial H_z}{\partial x}=(\sigma+\varepsilon\frac{\partial}{\partial t})E_y$$

(7) $$\frac{\partial H_y}{\partial x}-\frac{\partial H_x}{\partial y}=(\sigma+\varepsilon\frac{\partial}{\partial t})E_z$$

(8) $$\frac{\partial E_y}{\partial z}-\frac{\partial E_z}{\partial y}=(s+\mu\frac{\partial}{\partial t})H_x$$

(9) $$\frac{\partial E_z}{\partial x}-\frac{\partial E_x}{\partial z}=(s+\mu\frac{\partial}{\partial t})H_y$$

(10) $$\frac{\partial E_x}{\partial y}-\frac{\partial E_y}{\partial x}=(s+\mu\frac{\partial}{\partial t})H_z$$

If magnetic loss is not considered, set s=0, then, the above Maxwell's Equations are equivalent, and a full three-dimensional problem is thus formed.

FDTD algorithm is a numerical solution of Maxwell's Equations, which solves the propagation and reflection of electromagnetic waves in medium through difference handling of Maxwell's Equations, with the following basic approaches: regional space nodes are calculated adopting Yee cell method with FDTD, and Maxwell curl equations are dispersed using central-difference approximation, and then calculated using zigzag sampling.

The solution space is divided into several grid cells upward along three axes of coordinates. Δx、Δy and Δz are used to denote lengths of the cell along three axes, respectively, with Δt representing time increment. The coordinates of vertex of the grid cell（x,y,z）are noted as follows:

(11) $$(i,j,k)=(i\Delta x,j\Delta y,k\Delta z)$$

The function of any space and time can be expressed as follows:

(12) $$F^n(i,j,k)=F(i\Delta x,j\Delta y,k\Delta z,n\Delta t)$$

i,j,k and n are integers; the partial derivative of function to time and space is expressed as follows using central finite difference equation:

(13)
$$\frac{\partial F^n(i,j,k)}{\partial x}=\frac{F^n(i+1/2,j,k)-F^n(i-1/2,j,k)}{\Delta x}+O(\Delta x^2)$$

(14)
$$\frac{\partial F^n(i,j,k)}{\partial t}=\frac{F^{n+1/2}(i,j,k)-F^{n-1/2}(i,j,k)}{\Delta t}+O(\Delta t^2)$$

Yee cell that reflects the spatial arrangement of various nodes in electric and magnetic field in FDTD dispersion is shown in Figure 1.

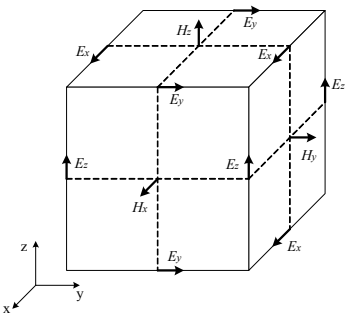

Fig .1. Yee cell in FDTD

It can be seen from the figure 1 that each magnetic field component is encircled by four electric field components; likewise, each electric field component is encircled by four magnetic field components. Moreover, zigzag sampling is performed on electric and magnetic field in line with time sequence during the calculation, and the time interval is half of a time step during the sampling, so as to form explicit difference equation after the dispersion of Maxwell's curl equations to perform iteration solution temporally. Therefore, with the initial value of electromagnetic problem given, the distribution of electromagnetic field at each time moment and space can be obtained step by step using FDTD algorithm.

Measured signals of current in GIS partial discharge

In this study, combining the measured PD current in GIS and experimental results obtained by other scholars, PD current signal with five defects including free metal particles, metal projection of high-voltage conductor, surface uncleanness of insulator, air gap of insulator and clearance of insulator is used as excitation source (signal waveform shown in Figure 2 to Figure 4), to study the propagation properties of electromagnetic waves.

a) free metal particles b) metal projection

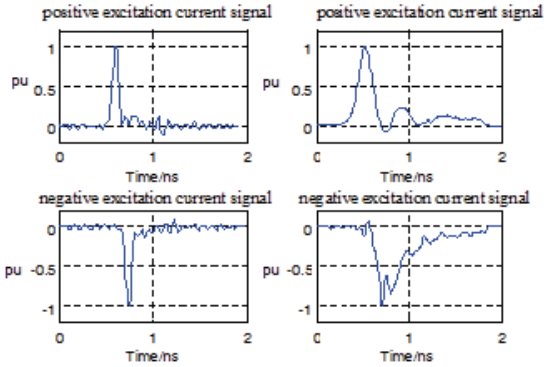

Fig . 2 Signal waveforms of PD pulse current with two typical defects in GIS

a) surface uncleanness of insulator b) air gap of insulator

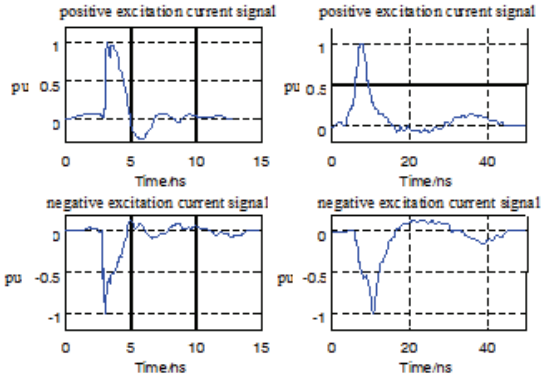

Fig .3. Signal waveforms of PD pulse current with two typical defects in GIS

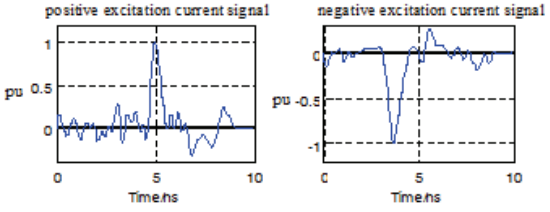

Fig .4. Signal waveforms of PD pulse current with defects of clearance between GIS insulator and conductor

It can be seen from the figure that great difference exists between PD current pulse in GIS and ideal Gaussian pulse. For different insulation defects, great discrepancies appear among measured PD current waveforms in terms of rising time, pulse width and pulse form under different discharge conditions. This indicates that partial discharge cases caused by different insulation defects possess different discharge mechanisms, resulting in distinction among electromagnetic waves excited by them. It can be inferred that the application of distinction among UHF PD signals can differentiate different types of insulation defects, thus providing theoretical basis for recognition of discharge source pattern based on UHF PD time domain signals. XFDTD is high-frequency electromagnetic simulation software developed by Remcom company in America, and it adopts FDTD algorithm to solve Maxwell's Equations, with its application of frequency scope of 100kHz~3000GHz. With user-defined interface at excitation source, signal data can be manufactured into .src source file according to the required format, thus the introduction could be performed.

Propagation properties of electromagnetic waves using measured signal of current as excitation source in GIS partial discharge

252kV GIS connection tube manufactured by SIEMENS high-voltage switch company is used as simulation computational model in this study, as shown in Figure 5, with the diameter of internal conductor of 180mm, internal diameter of outer shell of 398mm, and the length of a single connection tube of 1500mm. First, the modeling of two connection tubes and a disc insulator is conducted using 3D solid drawing software Pro/E, with flanges and lead angles adopted at each connection point, and its size is kept consistent with that of the real object. Then, IGS model constructed with Pro/E is introduced to XFDTD, and the material properties are set as follows: relative permittivity of insulator $\varepsilon = 4$; conductivity is 0; conductor and outer shell are both perfect electric conductors; boundary conditions are PML（Perfectly Matched Layer-PML） absorbing boundary; subdivision size of cell is 4×4×4mm; and the corresponding simulation signal frequency, simulation step, and simulation time duration is 7.49GHz, 7.7ps and 23ns, respectively.

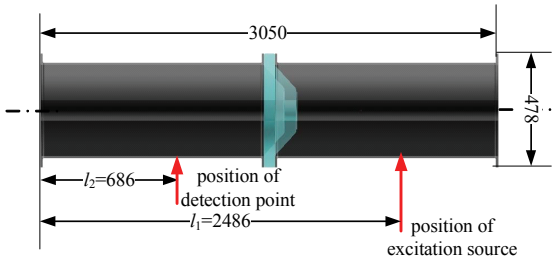

Fig . 5. Simulation computational model and settings of GIS

PD current signal of free metal particles is generated into excitation source .src file, as shown in Figure 2 (a), and XFDTD is introduced as self-defined excitation source that is located near Cell (83, 35, 380) of the bottom of GIS shell, i.e. l1=2486mm, where PD of free metal particles is likely to occur and where Cell (X, Y, Z) represents subdivision unit. The comparison is made with ideal Gaussian signal of the same pulse width. The detection point is located at Cell (83, 35, 80), i.e. l2=686mm, and the output quantity is the radial field intensity component EX at this point. In order to avoid the influence of electromagnetic wave reflection, the two ends of GIS tube are set to be two openings.

The simulation results are shown in Figure 6, where radial field intensity and the corresponding frequency spectrum of the detection point under PD positive and negative current pulse excitation of free metal particles, and ideal Gaussian pulse excitation of the equal width, are given, respectively. Apparently, the similarity between measured PD current main pulse and ideal Gaussian pulse in waveform is good. However, they differ in field intensity amplitude, resonance attenuation time and frequency spectrum, with the amplitude and resonance attenuation time of the latter being smaller than those of the former, while relatively small attenuation of each frequency component occurs during the propagation of electromagnetic waves.

a) Positive pulse excitation b) Negative pulse excitation c) Ideal Gaussian pulse excitation

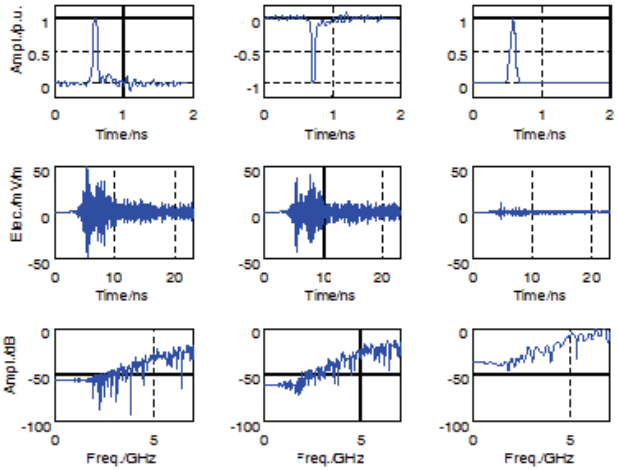

Fig. 6. Simulation results of PD current excitation of free metal particles

a) Positive pulse excitation b) Negative pulse excitation c) Ideal Gaussian pulse excitation

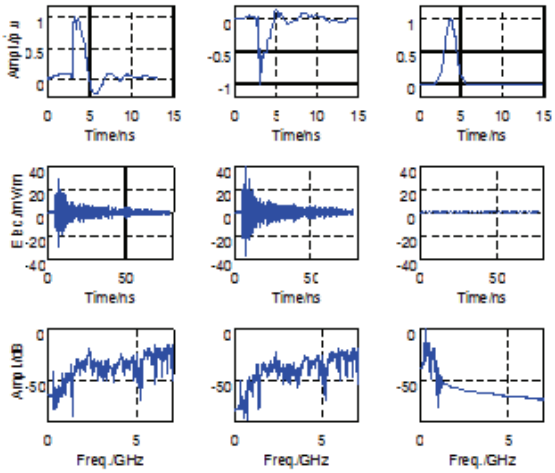

Fig.7. Simulation results under PD current excitation of surface uncleanness of insulator

Next, PD current signal with surface uncleanness of insulator is used as excitation source, as shown in Figure 3 (a), and the comparison is made with that under ideal Gaussian signal excitation of equal pulse width. The simulation time is set as 80ns, with the other settings being the same as what has been mentioned above, and the simulation results are shown in Figure 7. It can be seen that in spite of the equal pulse width, due to the bilateral asymmetry of the former, the rising edge is very steep, and the high-frequency components of electromagnetic wave excited are large in number, while the low-frequency components are few; the field intensity amplitude under ideal

Gaussian pulse excitation is very small, and the resonance attenuation time is long. By comparing Figure 6 and Figure7, it can be known that significant distinction exists in envelope and frequency spectrum of electromagnetic wave excited by partial discharge of surface uncleanness of insulator and free metal particles, indicating that for the same GIS structure, different electromagnetic waves are excited by excitation current with different waveforms.

This study aims to illustrate that electromagnetic waves excited by actual current in GIS partial discharge is not identical with ideal Gaussian pulse, and the electromagnetic waves excited by partial discharge caused by different insulation defects are also different. Therefore, the conduction of simulation research is confined to the two defects of free metal particles and surface uncleanness of insulator, without detailed explanation on other defects.

Influence of actual structure of GIS on the propagation of electromagnetic waves

At present, simplified GIS simulation model is adopted in the researches on propagation properties of electromagnetic waves in GIS in relative literatures, without considering the influence of radian of basin type insulator, three-phase common enclosure, shielding electrodes and breaker gas chamber, etc. Therefore, the emphasis of this section is placed on the influence of actual internal size and structure of GIS on the propagation of electromagnetic waves.

Influence of basin type insulator on the propagation of electromagnetic waves

GIS simulation models constructed in current research literatures mostly adopt disc insulators, while basin type structure is applied when the voltage is 252kV or above, as shown in Figure 8 (a). In terms of refraction, reflection and attenuation of electromagnetic waves, there is a disparity between basin type and disc-shaped insulator.

a) 252kV GIS basin type insulator

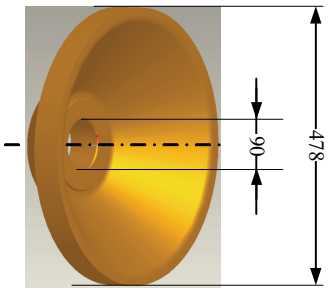

b) GIS simulation computational model and the settings

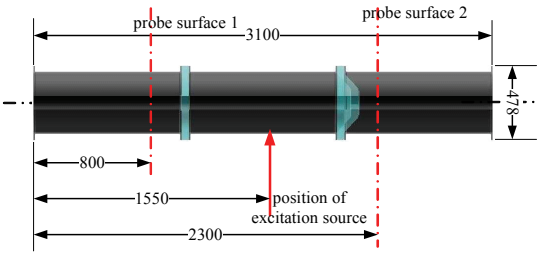

Fig.8. Basin type insulator and GIS simulation computational model

252kV GIS manufactured by SIEMENS Company is taken as an example of GIS simulation computational model. As shown in Figure 8 (b), a disc-shaped insulator and a basin type insulator are used to connect three GIS connection tubes, with the diameter of internal conductor of 180mm, internal diameter of outer shell of 398mm, length of a single tube of 1000mm, and the thickness of insulator of 50mm. PD positive current signal of GIS conductor metal projection shown in Figure 2 (b) is adopted as excitation source, with the following settings: located at Cell (83, 70, 409); two detection points Cell(84, 37, 234) and Cell(84, 37, 585) are located at the bottom of two probe surfaces with equal distance to excitation source; simulation time duration is 43ns; output quantity is radial field intensity component EX at detection point and the distribution of field intensity at two probe surfaces; other simulation settings are identical with those in Section 2.

Simulation results are shown in Figure 9 and Figure 10. Figure 9 is the field intensity and frequency spectrum at detection point; it could be known by comparison that the attenuation speed of electromagnetic waves passing through disc-shaped insulator is faster, and the reflection of electromagnetic wave is greater, while the attenuation of various frequency components of basin type insulator is greater. Figure 10 shows the field intensity distribution at the same moment at the two probe surfaces. It can be seen that it takes shorter time for the wave head of electromagnetic wave passing through disc-shaped insulator to arrive; the electromagnetic wave passing through disc-shaped insulator propagates along high-voltage conductor from the bottom to the top, while that passing through basin type insulator propagates along the inner wall of GIS shell from the bottom to the top; the regional distribution of field intensity at probe surface 1 is relatively concentrated, while that at probe surface 2 is relatively homogeneous.

a) disc-shape b) basin type)

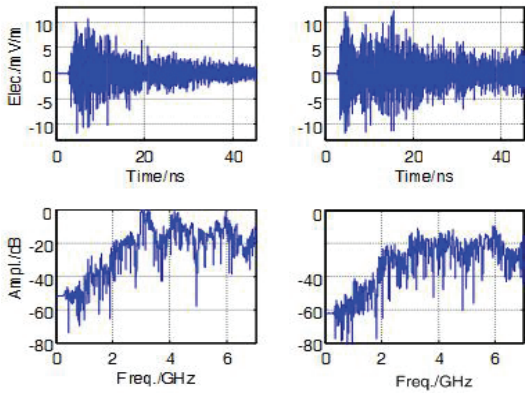

Fig. 9. Simulation results of the influence of basin type insulator on the propagation of electromagnetic waves

a)disc-shape

b)basin type

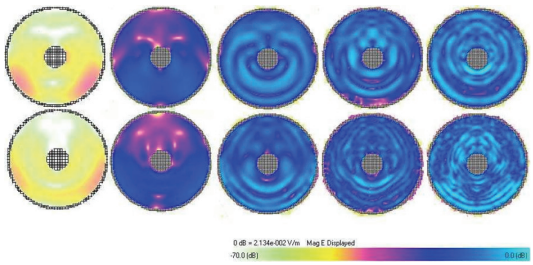

Fig.10. Comparison on field intensity between probe surface 1 and probe surface 2

It can be found through above simulation research and analysis that the differences exist in the influences of basin type insulator and disc-shaped insulator on propagation of electromagnetic waves. The disparity in attenuation properties, reflection properties, propagation direction of electromagnetic waves and field intensity distribution deserves the attention during UHF PD detection, pattern recognition and positioning of discharge source.

Influence of shielding electrode on the propagation of electromagnetic waves

a)252kV GIS shielding electrode

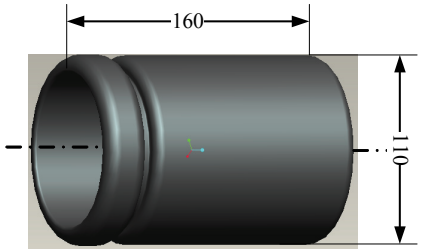

b) Schematic diagram of the installation of shielding electrode

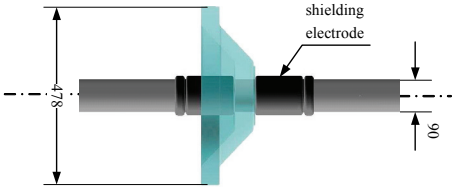

Fig.11. Shielding electrode and the schematic diagram of its installation

a) without shielding electrode b) with shielding electrode

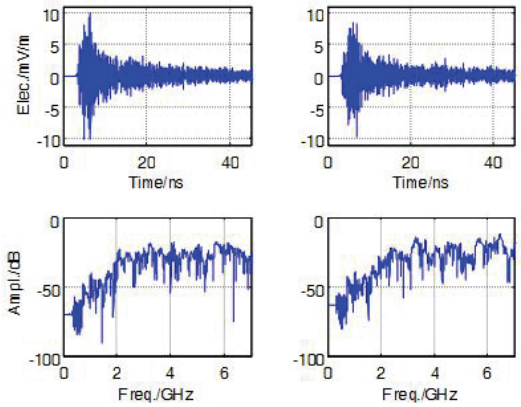

Fig.12. Simulation results of the influence of shielding electrode on the propagation of electromagnetic waves

In order to obtain homogeneous field intensity and increase curvature radius of electrode in the actual structure of GIS, shielding electrodes are installed at conductor joints, corners and the two sides of isolation insulator, etc. As a metal component in GIS, the presence of shielding electrodes will give rise to attenuation, reflection and refraction of electromagnetic waves. 252kV GIS shielding electrodes and GIS model installed are shown in Figure 11, with the length of shielding electrode of 160mm, internal diameter of 90mm, and external diameter of 110mm. The positions of simulation computational model, excitation source, and detection point are shown in Figure 5, and the setting are as follows: the simulation time duration is 43ns; output quantity is radial field component EX at detection point; other settings are identical with those in Section 2. The simulation is conducted with and without shielding electrodes, respectively.

Simulation results are shown in Figure 12. It can be seen the envelope shapes of resonance attenuation of UHF PF signals are basically identical with or without shielding electrodes; the attenuation of signal amplitude occurs somewhat with shield electrodes, while the frequency spectrum without shielding electrodes is smooth. However, the case when only one pair of shielding electrodes is used is investigated in this study. In practice, several shielding electrodes might be installed at the conductor joints, corners, the two sides of isolation insulator of GIS, with their influence on the propagation of electromagnetic waves being non-negligible.

Propagation of electromagnetic waves in GIS with three-phase common enclosure

a) GIS with one-phase single enclosure b) GIS with three-phase common enclosure

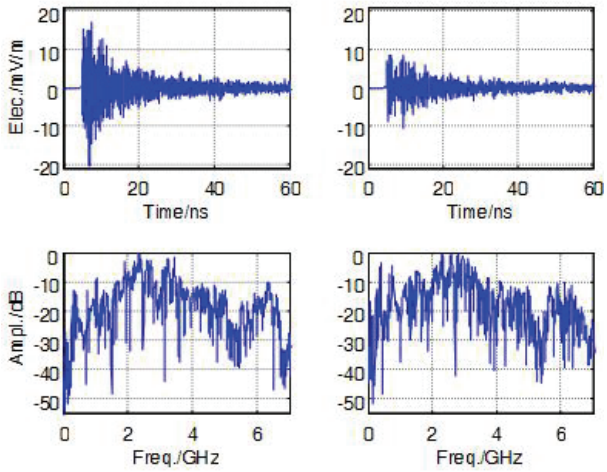

Fig. 13. Simulation results of propagation of electromagnetic waves in GIS with three-phase common enclosure

For GIS with voltage of 252 kV or above, installation method of one-phase single enclosure is frequently used, while for GIS with voltage of 126kV or below, that of three-phase common enclosure is adopted. In order to study the difference in propagation of electromagnetic waves under these two situations, two GIS simulation computational models are constructed, respectively, as shown in Figure 5; one is one-phase single enclosure, and the other is three-phase common enclosure. With their conductors, diameters of outer shells, and simulation settings being identical, the simulation computation is then carried out, respectively. The specific settings are as follows: excitation source is located at Cell (83, 70, 80); the detection point is located at Cell (37, 83, 120); the simulation time duration is 60ns; output quantity at detection point is radial field intensity component EX; other simulation settings are identical with those in Section 2.4.1.

Simulation results are shown in Figure 13 and Figure 14. It can be seen from the comparison on Figure 13 (a) and (b) that the attenuation amplitude and low-frequency component of electromagnetic waves are relatively great in GIS with three-phase common enclosure. Figure 14 shows the field intensity distribution of probe surface xy plane: z=120. Apparently, the wave head of electromagnetic wave in GIS with one-phase single enclosure mainly propagates along the periphery of conductor, while that in GIS with three-phase common enclosure mainly along the middle of three conductors, with relatively long time for resonance attenuation.

a) one-phase single enclosure

b) three-phase common enclosure

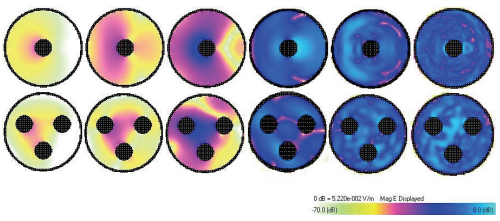

Fig.14 . Comparison on the field intensity distribution on probe surfaces

Propagation of electromagnetic waves in GIS breaker

Breaker is one of the most integral and structurally complex components in GIS, where insulation faults frequently take place. GIS breaker for 126kV three-phase common enclosure manufactured by Zhengtai High-voltage Switch Company is taken as an example for the investigation on the propagation and diffusion of electromagnetic waves in GIS breaker.

a) Internal structure diagram of 126kV GIS breaker model

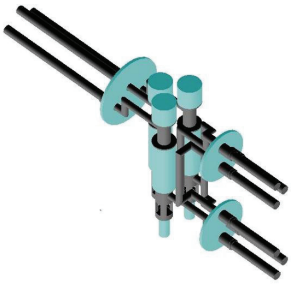

b) Appearance diagram of 126kV GIS breaker model

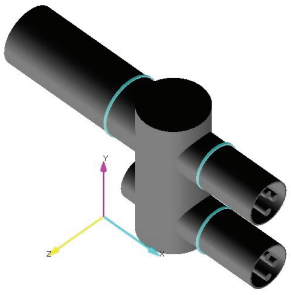

Fig.15 . 126kV GIS breaker model

a)Front view of 126kV GIS breaker model

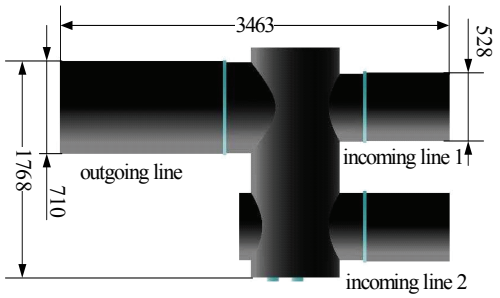

b)Schematic diagram of the position of excitation source and detection points

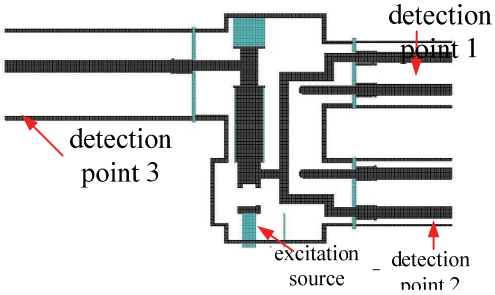

Fig.16. Schematic diagram of the size of 126kV GIS breaker and the positions of detection points and excitation source

3D solid model with the same size and structure to real object is first constructed applying Pro/E software, as shown in Figure 15. Its size is shown in Figure 16 (a), and the positions of excitation source and detection point are shown in Figure 16 (b), where the part in dark color is metal conductor and GIS shell, while that in light color is epoxy insulator. PD current positive pulse of insulator air-gap shown in Figure 3 (b) is used as excitation source, located at Cell (152, 32, 49); detection point one is located at Cell (240, 95, 49); detection point two at Cell (240, 50, 63); and detection point three at Cell (50, 90, 49); the radial field intensity distribution, i.e. xy plane: z=49 is output simultaneously. Simulation precision and computation time should also be considered: simulation step length is 28.8875ps; grid subdivision is Cell 15×15×15mm; maximum signal frequency of simulation is 2GHz. Since the rising edge of excitation source adopted is not very steep, the requirement on simulation signal frequency can be satisfied.

Simulation results are shown in Figure 17 and Figure 18, and the following can be known from the waveforms in figures.

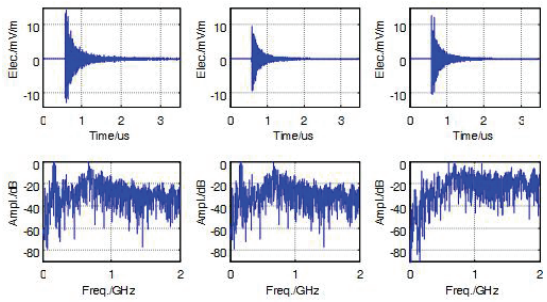

Fig.17. Simulation results of electric fields and its frequency spectrum of the detection points

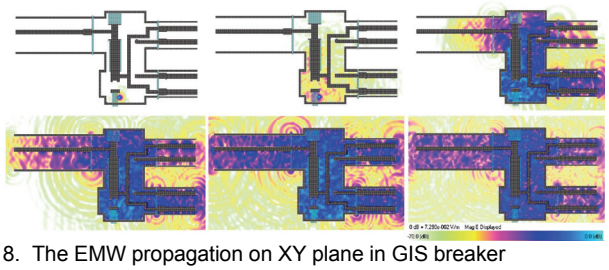

Fig.18. The EMW propagation on XY plane in GIS breaker

(1)Because of the complex internal structure of cavity of breaker, the reflection and refraction of electromagnetic waves occur; the resonance attenuation time of radial electric field is 1-1.5us at the three detection points, being much longer than that in the aforementioned simulation result.

(2) Although detection point one and three are more distant away from discharge source than detection point two, their signal amplitude is larger as a result of superposition of reflected waves. This indicates that UHF signal amplitude is not necessarily proportional to its distance to discharge source in the complex structure of GIS.

(3)Compared with detection point three, low-frequency components of 1GHz or below are more in detection point one and two, while high-frequency components are less. However, according to the simulation results of GIS model with one-phase single enclosure in the literatures, the proportion of frequency components is supposed to be inversely proportional to the diameter of GIS shell, which is just contrary to the simulation results in this study. This indicates that the propagation properties of electromagnetic waves are different in the simple or complex structure of GIS.

(4)The propagation, diffusion, reflection and resonance of electromagnetic waves in the breaker can be clearly seen from Figure 18, and the electromagnetic waves leaked from the insulator can be applied in external UHF PD detection.

Conclusion

The discharge in medium is the accumulation and release of electric field energy in the form of charge accumulation and electron motion, and partial discharges caused by different insulation defects also vary, with the disparity existing in electromagnetic waves excited. In this study, with actual GIS PD current signal taken as excitation source, the influence of actual structure of GIS on the propagation of electromagnetic waves is studied. The results show that great difference occurs between electromagnetic waves excited by PD actual current signal and that by ideal Gaussian pulse excitation; it has been pointed out that basin type insulator, shielding electrodes and three-phase common enclosure can affect the amplitude, frequency component and propagation mode of electromagnetic waves. When electromagnetic waves propagates in GIS breaker, the time duration for signal resonance attenuation is relatively long, and the signal intensity is not necessarily proportional to its distance from discharge source; the proportion of frequency components is proportional to the diameter of GIS shell.

Acknowledgment

The financial support from The Science and Technology Commission of Shanghai under Grant No. 10dz1203000 is gratefully acknowledged.

REFERENCES

[1] T. Hoshino , K. Kato , N. Hayakawa et al, "Frequency Characteristics of Electromagnetic Wave Radiated from GIS Apertures," IEEE Transanctions on Power Delivery, vol. 16, pp. 552-557, April 2001.

[2] M. Hikita, S. Ohtsuka, T. Teshima, et al, "Electromagnetic (EM) Wave Characteristics in GIS and Measuring the EM Wave Leakage at the Spacer Aperture for Partial Discharge Diagnosis," IEEE Transactions on Dielectrics and Electrical Insulation, vol. 14, pp. 453-460, Feb. 2007.

[3] J. Qin, C. C. Wang, and W. M. Shao, "Applying UHF to Partial Discharfe Online Monitoring of Electric Apparatus," Power System Technology, vol. 21, pp.33-36, Mar.1997.

[4] S. Okabe, S. Yuasa, S. Kaneko, et al. "Simulation of Propagation Characteristics of Higher Order Mode Electromagnetic Wave in GIS," IEEE Transactions on Dielectrics and Electrical Insulation. Vol. 13, pp.855-861, August 2006.

[5] M. Yoshimura, H. Muto, C. Nishida, et al, "Propagation Properties of Electromagnetic Wave through T-branch in GIS," IEEE Transactions on Dielectrics and Electrical Insulation , vol. 14, pp. 328-333, April 2007

[6] M. Hikita, "Examination of Electromagnetic Mode Propagation Characteristics in Straight and L-Section GIS Model Using FD-TD Analysis," IEEE Transactions on Dielectrics and Electrical Insulation, vol. 14, pp. 1477-1483, Mar. 2007

[7] S. Okabe, and S. Kaneko. "Electromagnetic Wave Propagation in a Coaxial Pipe GIS Model," IEEE Transactions on Dielectrics and Electrical Insulation, vol. 14, pp. 1161-1169, Mar. 2007.

Qin Li *(1965-), male, professorate senior engineer, His research interests are in online monitoring electrical apparatus of electrical measuring technology and automatic control&monitor of power system.*

Wubing Qiu *(1964-), male, professorate senior engineer, His research interests are in control of power system.*

Kaisui Cai *(1958-), male, senior engineer, His research interests are in online monitoring electrical apparatus of electrical measuring technology and automatic control&monitor of power system.*

Gehao Sheng *(1974-), male, associate professor, His research interests are in the key technologies in intelligence transmission line& online monitoring electrical apparatus.shenghe@sjtu.edu.cn.*

Yadong Liu *(1982-), male, doctoral candidate His research interests are in the key technologies in intelligence transmission line& online monitoring electrical apparatus.lyd@sjtu.edu.cn*

Xingquan Huang *(1959-), male, associate professor, His research interests are in online monitoring electrical apparatus of electrical measuring technology and automatic control&monitor of power system.*

Xiuchen Jiang *(1965-), male, professor His main research fields are in electrical measuring technology and electrical apparatus automation. jiangxiuch@163.com.*